SURVEILLANCE SYSTEM
AIRBORNE COMPOSITE RADOME DESIGN

G. Pulvirenti (1) , P.D.Tromboni (1), M. Marchetti (1), A.Delogu (2), A.Maccapani (2), R.Aricò (3)

(1) Dip.Ing. Aerospaziale ed Astronautica, Università di Roma "La Sapienza" - Italy

(2) Galileo Avionica (TO) - Italy

(3) Sistema Compositi , Castellaccio di Paliano (FR), Italy

Tel. +39 06 44585800; mail: mario.marchetti@uniroma1.it

ABSTRACT

A prototype F100 aircraft will be equipped with an experimental ground surveillance radar system based on the use of electronic beam steering, moving target identification (MTI) and synthetic aperture imaging.

The Airborne Radome is a structure that serves to enclose a radar antenna and to protect it from its physical environment. There are a wide variety of Radome types, and they can be placed on different parts of the aircraft, making its design different for each case. The antenna of the surveillance radar system is housed in an oblong radome underneath the fuselage, located just forward of the wing.

The conception of such a unit is subjected to electrical and structural requirements, because of this, materials used for airborne radomes must have electrical and high mechanical strength properties, but unfortunately, this properties are often mutually exclusive and a compromise solution must be adopted.

The scope of this paper is to present a review of a complete radome design, beginning from the electrical design, studying material options, analyzing and determining a wide range of mechanical loads, to finish with structural verifications, as bird impact numerical analysis and mechanical material testing .

Also a brief description of the FEM model, strength and failure criteria are developed on this work.

1 INTRODUCTION

Radome is an acronym taken from radar-dome, and is the structure that serves to enclose a radar antenna and to protect it from its physical environment (rain, winds, ice, aerodynamic pressure), and must be adapted to the aerodynamics of the fuselage.

There are a wide variety of Radome types, and they can be placed on different parts of the aircraft, making its design different for each case. For example, most common large aircraft radomes typically form the nose or tail cone of the aircraft, or they can be flush mounted or sited on the leading or trailing edges of a wing, fuselage or tail fin. This paper is based on an airborne radome located underneath the fuselage, and just forward the wing which houses a ground surveillance radar system.


Fig.1- Global express jet - ASTOR


Fig.2- Nose radome

The conception of such a unit is subjected to electrical requirements of the radar such as high transmission, low reflection, far-field radiation pattern, power transmittance, low absorption and small bore sight errors among others. The requirements may be meet by the selection of the appropriate materials and by maintaining the correct wall thickness.

Fig.3 -Kaman S2HF Radome

Materials used for airborne radomes must have low dielectric constant and high mechanical strength, but unfortunately, low dielectric constant and high mechanical characteristics are often mutually exclusive and a compromise solution must be adopted. Organics materials are used in most aircraft radomes but they are not the best solution for high temperatures (higher speeds), where ceramics are used.
Definition of shape is mainly influenced by radar mission and aerodynamics, and the choice of materials and wall thickness must satisfy structural strength , electrical performance, low weight, thermal stability and rain erosion requirements. Radome size is controlled by aircraft dimensions, it is desirable to use as large a radome as aircraft permits, since bore sight error is reduced as the antenna size increases.

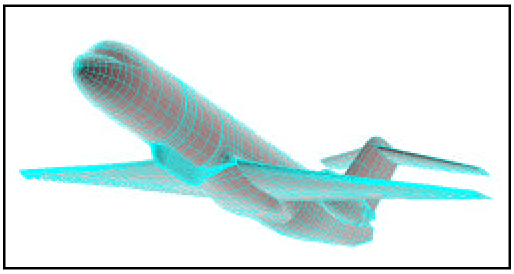
Fig.4- Case study radome location

2 MATERIALS AND GEOMETRY

2.1 Radome wall geometry and construction considerations

Wall construction presents two principal options to considerate; solid or sandwich walls; the former is associated to high speed performances, and the second kind to lower speed and less mechanically demanding applications.

Principals characteristics are the following:

→ Solid walls (half wavelength thickness wall)

- Wide use
- Electrically simple design
- Reasonable transparency over different incidence angles
- Narrow operational bandwidth

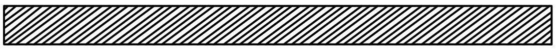

Fig.5 Solid laminate

→ Sandwich (simple, multiplayer)

A) Simple wall :

- Low density, low dielectric core with skins of higher dielectric constant
- Relatively broadband
- Flexible design

Fig.6 Simple sandwich

B) Multi-layer wall

- Radome wall having more layers to meet the need for increased operating frequency bandwidth, increment structural stiffness an reduced weight.

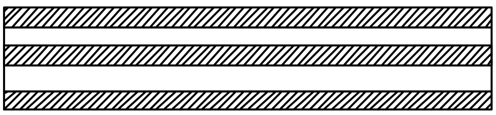

Fig.7 Multilayer sandwich

2.2 Materials

Radome applications require materials which offer high specific mechanical properties coupled with good dielectric characteristics, this electrical performance may be achieved by using RF transparent materials.

Materials can be simply divided into two categories **[1]**;

Non-Organic materials
-Heat resistant to high temperature
-Used in hypersonic missiles
Organic materials
-Used in most radomes
-Mechanical strength deteriorates at high temperatures
Solid wall and higher dielectric constant skin material of sandwich radomes is generally made of resins incorporating reinforcement fibres.
Glass or aramid fibres composites are preferable. Electrically conducting reinforcements, such as carbon or boron are absolutely not viable.
Aramid composites have electrical properties that make them of interest for RF transparent structures. The electrical properties are the following [2]:

→ Relative dielectric constant (ε_r)
→ Loss Factor (tan d)

A Materials comparison can be seen in the following table.

Reinforcement / resin	Relative dielectric constant	Loss Factor
E-glass / Epoxy	4.4	0.016
E-glass / Polyester	4.15	0.015
D-glass / Polycianate	3.45	0.009
Kevlar / Polyester	3.5	0.012
Quartz / Epoxy	3.12	0.011
Ceramics, Alumina	9.6	0.0001

Table 1. Materials comparison

The main disadvantage of Kevlar is the high tendency to moisture pick-up, which can be avoided using appropriate protections
Quartz was considerate but dis carded because of it's high cost and low structural performance.

3 CASE STUDY, RADOME REQUIREMENTS & DESIGN CRITERIA

The prototype Q1 of the F100 will be equipped with an experimental ground surveillance radar system. The antenna of the radar system is housed in an oblong radome underneath the fuselage, located just forward of the wing.

Fig.8 Pictorial view of aircraft / radome

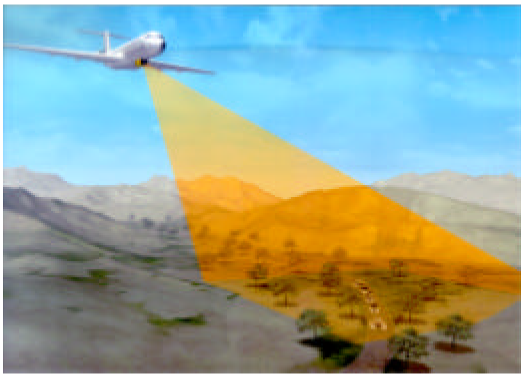

Fig.9 Ground surveillance

For easy manufacturing and maintainability, the radome shall be manufactured and studied in three isolated parts. The front and rear parts (fairing) have only aerodynamic and structural functions and are not required to be electrically transparent, and as a first approach will be studied as a E-glass/Epoxy mono-skin structure. The two fairings include a lightning protection system with a metallic mesh on the outer surface of the laminate.

On the other hand, the central part of the Radome must be electrically transparent (since directly illuminated by the radar antenna). After an "electrical study" of the central part, an initial wall configuration was defined, featuring a multi-layer sandwich made of Nomex core and Kevlar skins.

Fairings and central part will be joined by two bolted Aluminum T-Ribs (Fore and rear "T" ribs) to guarantee structural stiffness and to provide grounding points for the lightning protection system. The radome and fairings are connected to the fuselage of the aircraft through a bolted mounting profile.

As can be seen in figure 10 , radome structure is divided in three sections;

1. Forward fairing (E-glass mono-skin, one meter long).
2. Mid section (Kevlar-Nomex multi-layer sandwich, three meters long).
3. Aft fairing (E-glass mono-skin, one and a half meters long).

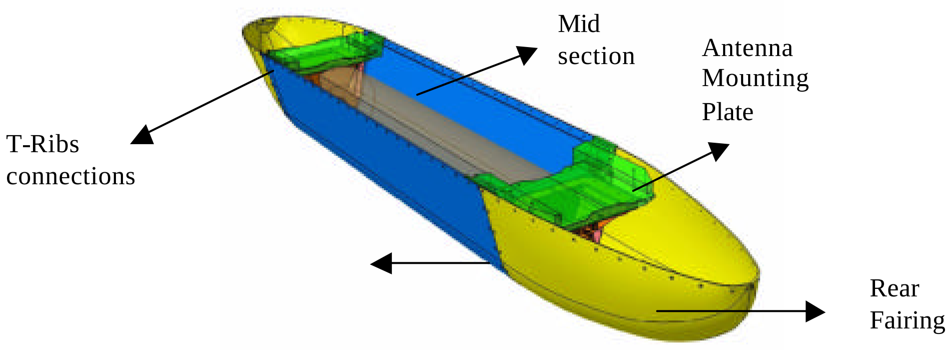

Fig.10 Radome parts

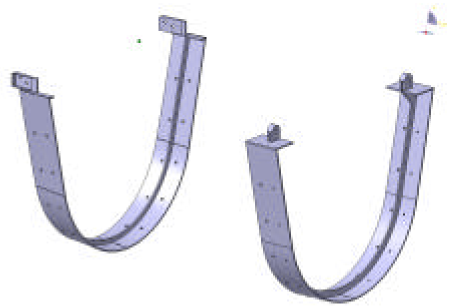

Fig.11 Connection brackets

3.1 Materials

The following steps were carried out to conduct the electrical design:

-Definition of materials and wall configuration
-Initial definition of wall thickness
-Electrical performance analysis and optimization.
-Final performance analysis.

All this steps were performed in strict correlation with the structural design in order to guarantee total compliance.
As mentioned before a multilayer structure was selected because it presents a good performance over a much larger bandwidth (in frequency and in terms of incidence angle), a good structural performance and relatively low weight.
In comparison with the multilayer configuration, other structures were analyzed :
-A monolithic configuration was discarded because of higher weight and lower electrical performance.
-A simple sandwich (3 layers) was discarded because of relatively poor structural and electrical performance.

Radome wall thickness has been initially defined using a theoretical model which computes the transmission and reflection coefficients of a planar multi-layer planar structure illuminated by a planar wave front. Then analysis and design refinement on a complete radome model has been performed using dedicated computer code.
Wall has been assumed to present a constant thickness in all planes: the use of a non constant thickness design would not justify the effort and the manufacturing complication necessary to produce such radome wall configuration.

3.2 Design Loads

3.2.1 Static & Dynamic analysis

In the static analysis five basics loads are considered, and different combinations of them are studied creating in this way fourteen “Load cases”.
Basic loads are the following:

a) Symmetrical Cp distribution
b) Asymmetrical Cp distribution
c) Water Spray loads
d) Inertial Loads
e) Rapid decompression
f) Bird Impact

- Loads Description

To calculate the Aerodynamic limit loads, the following cruise speed was selected, with this input was possible to develop a software to determinate the pressure distribution along the radome;

Speed (KEAS) = 350 (Mach 0.80)
Altitude = 17000 feet
V_∞ = True air speed; 200m/s
ρ_A = density of air; 0.6kg/m^3

- Symmetrical flight condition [5]

In order to maintain well into subsonic airflow conditions, the computations were not performed for the limit load condition, but these were done at Mach number of Mach 0.70 whereas the limit load condition is at Mach 0.84. After that, the results were converted with the ratio of the Prandtl-Glauert factor, eqn.(1), to the limit load Mach condition, resulting in a conservative Cp distribution:

$$(C_P)_{M0.84} = (C_P)_{M0.70} \times R_{PG} = (C_P)_{M0.70} \times \frac{1/\sqrt{1-0.84^2}}{1/\sqrt{1-0.70^2}} = (C_P)_{M0.70} \times 1.3162 \qquad (1)$$

- Asymmetrical flight condition [5]

Computations were performed to analyse the sideslip effect on the local pressure distribution of the radome. The computations were performed at Mach 0.50 for symmetrical conditions and repeated for -5 degrees of sideslip .In the results, angle of attack effects were nil and therefore only data for Alpha=0deg was used for analysis. The differences in $C_{P\,LOC}$ between the symmetrical and asymmetrical conditions were used to address the sideslip effect on the radome local pressure distribution and a correction factor must be added to the symmetrical flight condition, after that, the limit flight condition must be obtained with the Prandtl-Glauert factor.
To prevent accumulation of water inside the radome, and as a way to manipulate the internal pressure (an optimal load condition exists with a minimum pressure differential between internal and external pressure), a pair of drain holes should be drilled in the lowest part of the radome. Because of the drain holes, the external Cp distribution must be updated with the following formula:

$$(C_{P\,LOC})_{TOTAL} = (C_{P\,LOC})_{INTERNAL} + (C_{P\,LOC})_{OUTSIDE} \qquad (2)$$

On parts of the Aft fairing separated flow must be simulated applying a local CP=-0.6

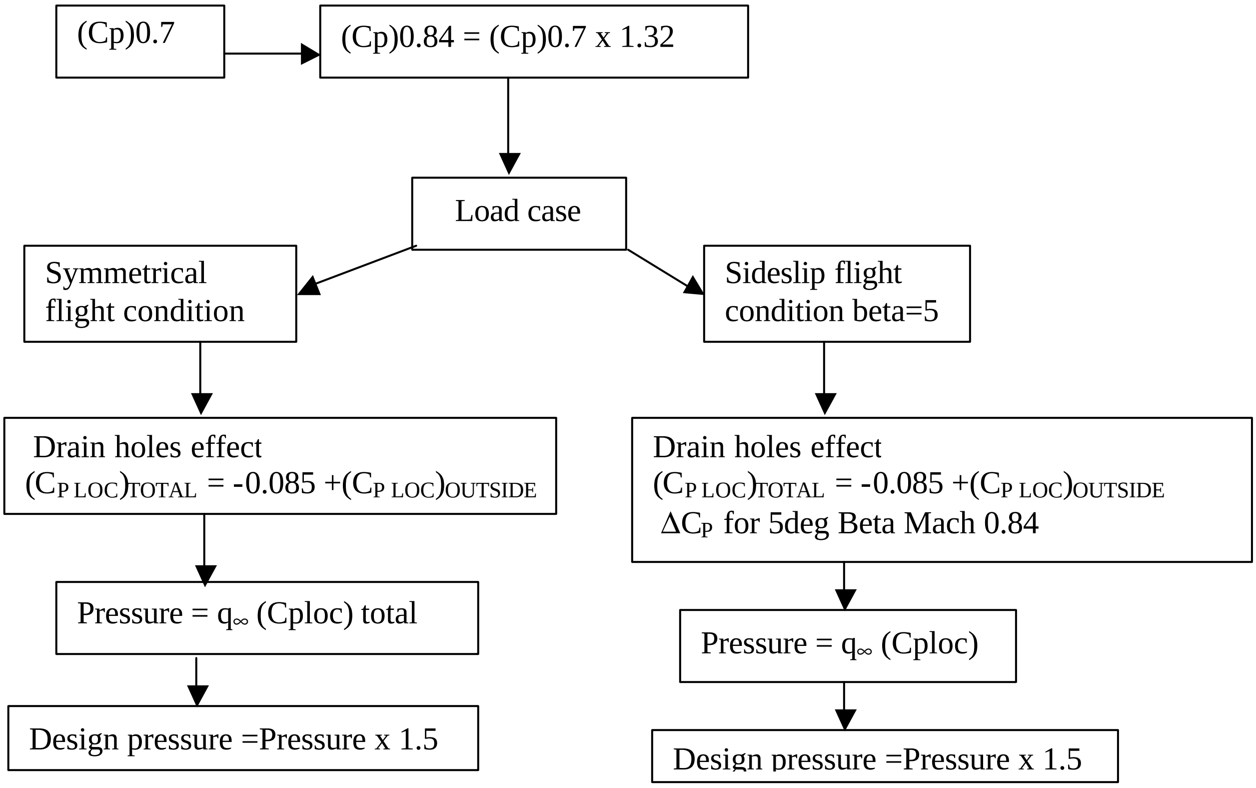

Table 2. Pressure Loads

- Water-spray loads [5]

If radome and aircraft must operate from runways with precipitation (up to 0.5-inch depth of water) this load must be taken into account.

During take-off from and landing on a precipitated runway, under some conditions water-spray from the nose wheel tyres may impinge on the forward fairing of the radome.

The sprays produced by aircraft tyres running in water or slush are complex and depend on ground speed, the shape and dimensions of the loaded tyre and the contamination depth. At low speeds, the quantity of water displaced by a tyre will depend on water depth, tyre cross-section and tyre forward velocity. The tyre remains in contract with the runway and displaces water forward (bow wave) and sideways (side spray). At the aquaplaning speed V_A the tyre looses contact with the runway and ceases to display water forward; all the displaced water will be sprayed sideways. Beyond V_A the amount of displaced water will reduce significantly, because the tyre will skid over the water.

The aquaplaning speed V_A is the velocity at which the kinetic pressure (of the water) equals the tyre contact pressure (tyre inflation pressure). V_A is dependent from the tyre inflation pressure and from the mass of the precipitation.

$$F_{WATER} = \frac{1}{2} \times \rho_{WATER} \times V_A^2 \times \text{water depth} \times \text{tyre width} \qquad (3)$$

- Inertial loads

The inertia loads shall be determined as follows: $F = m . g . n$ (4)
where:
F = inertia load [N], in the (same) direction of n;
m = items mass [kg];
g = gravitational constant ($g = 9.80665 = 9.81\ m/s^2$)
n = load factor in a certain direction [-]

- Decompression Loads

In case of an explosive decompression of the aircraft fuselage (i.e., a hole on the fuselage) , it is possible that the cabin pressure passes trough the fuselage to the radome (maximum pressure for the cabin is 7 psi) loading the radome with an high internal pressure. This is an emergency case, and because of this , emergency procedures must be taken into account (lower aircraft speed and altitude). To avoid Radome failure (with out penalizing "normal flight conditions" with a bigger safety factor) it is necessary to evacuate this high pressure air without radome destruction.
A wide range of possible solutions or configurations were studied, in the following list we can see the principal options:

1) To make a weak part on the aft fairing laminate in order to guarantee failure of the rear fairing at a pressure lower than the radome. However a very thin fairing wall should be used which is not compatible with other load cases. Moreover a "controlled" failure in a laminated structure is not easy to be designed.
2) To use a pair of membrane valves inserted on the after fairing laminate. This solution would require a high flow-rate valve which would make design critical.
3) Third solution was to incorporate fuse-bolted doors on the aft Fairing. In this way the bolts will fail under an established pressure value allowing air pressure to open the vent doors. With this solution no parts will blown-off from the aircraft avoiding dangerous impacts on aircraft structure or ground.

Solution number 3 was selected, and the next step was to determine the required size for the air flow area (venting doors) as a function of the overpressure.
After FEM simulations with different internal pressures (2,3,4,5,6 psi) we found that the central part of the radome was the first to fail. Analysing displacements and laminate failure index for each internal pressure case, the maximum overpressure was established in 4 Psi (with out radome failure).
Flow area determination can be seen in the following picture where for a failure differential pressure of 4psi a venting area of $0.2\ m^2$ is needed.

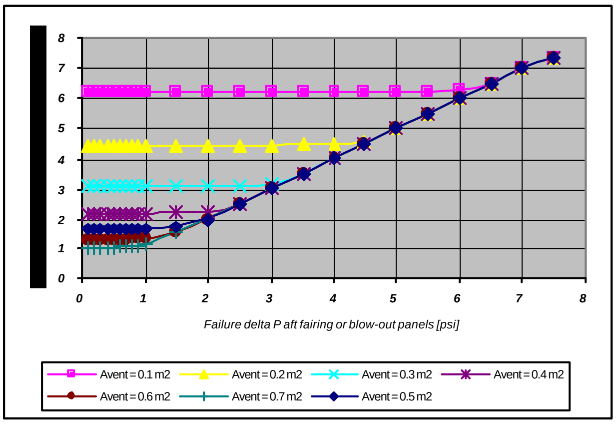

Fig.12 Explosive decompression pressure

The venting door configuration resulting from decompression analysis can be seen in the following picture.

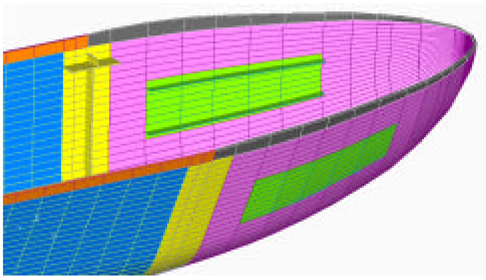

Fig.13 Laminated venting door

It is clear that after the “Explosive decompression” the aircraft must continue flying, so an “After Decompression " load case must also be considered.

- **Bird Impact**

In the event of a bird strike, the radome shall remain a complete shell and shall not endanger the flight safety. The requirement of JAR 25.631 must be applied: “…The structure must be designed to assure capability of continued safe flight and landing after impact with a 8 pound bird when the velocity of the airplane is equal to VC at sea level..”

A specific 3D numerical model has been realized to simulate the impact event. The numerical code SAMTECH PLEXUS® has been used to implement an explicit non linear analysis. The complete 3D model, which represents both the radome and the fairings structures, has been constrained (pinned) to the aircraft structure and has been meshed with 2D shell elements, using different materials properties for external fairings and radome respectively. The impacting bird has been simulated developing a specific property constituted by a group of interconnected nodes and using a viscoelastic material. The bird is composed by spherical non dimensional element with appropriate mass and behavior connected each other through controlled elastic connections. These are able to release the spherical nodes when an assigned energy level is reached during the impact process. In this way it is gradually possible transfer to the structure the impact energy, which depends on the initial relative velocity between the bird and the radome and also on the impact angle respect to the longitudinal axis in the symmetric plane of the structure.

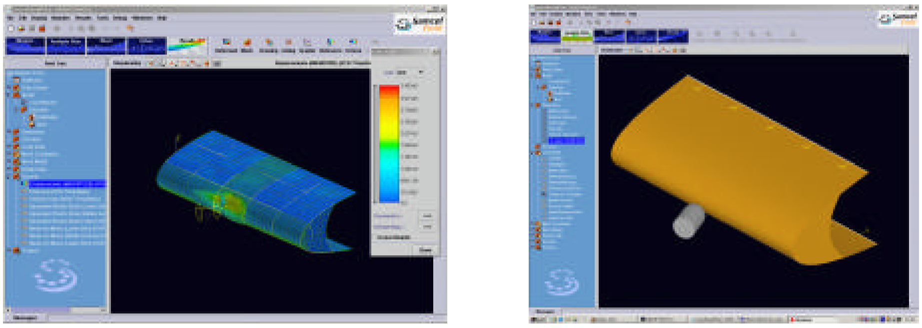

Fig.14- Bird impact simulation-SAMTECH PLEXUS®

3.3 Load Cases

A FEM static analysis was carried out on these all load cases, where a combination of Aerodynamics, inertial and water-spray forces are included.

LOAD CASE	Load	Inertial force direction
1	Symmetrical pressure distribution	Downward
2	Asymmetrical pressure distribution	Downward
3	--	Forward
4	--	Rearward
5	--	Sideward
6	--	Upward
7	--	Downward
8	Water Spray	Forward
9	Water Spray	Sideward
10	Water Spray	Upward
11	Water Spray	Downward
12	Water Spray	Afterward
13	Internal pressure (3psi)Limit AeroLoads (M0.77)	Downward
14	After decompression Limit Aero Loads (M0.27)	Downward

Table 3. Load Cases

After that, the most critical cases (2 and 13) were selected to perform a more detailed FEM analysis, including the venting bolted doors on the model, and spring stiffened connections to simulate radome- aircraft connection profile.

3.4 Strength and stiffness criteria

The radome structure must be designed so that material ultimate strength will not be exceeded at ultimate loads, understanding ultimate loads as limit loads multiplied by a factor of safety of 1.5. This allowable stresses must include the effects of material strength reduction due to action of moisture and exposure to temperature.
As a principal analysis parameter for laminate elements, the Hoffman [3] criteria failure is evaluated using eqn (5). This index takes into account normal and shear stresses on element as follows:

$$F(s_x, s_y, t_{xy}) = \frac{s_x^2 - s_x s_y}{X_t X_c} + \frac{s_y^2}{Y_t Y_c} + \frac{X_c - X_t}{X_c X_t} s_x + \frac{Y_c - Y_t}{Y_c Y_t} s_y + \frac{t_{xy}^2}{S^2} \qquad (5)$$

Where (X_t ,X_c) e (Y_t, Y_c) are the compressive and tensile stress limits and S represents the maximum allowable shear stress.
Another point to consider is Radome deformation. The cumulative effects of elastic and thermal deformation shall not cause any interference between radar antenna and Radome, under the worst condition, the inner surface of the radome must not come closer than 10mm to the nominal position of any part of antenna and other components.

4 FINITE ELEMENT MODEL

Finite element models are described by their topology , and their properties (material and elements).
The Radome was modeled using FEMAP- NASTRAN® software. The elements used are "laminate elements", this kind of element allows to characterize a layered composite (Fairings and mid section) and plate elements (T-rib profiles).

4.1 Laminate Element description

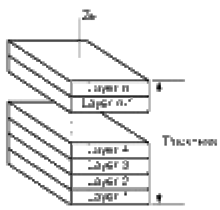

Fig.15- Laminate element

Similar to the plate element, except that this element is composed of one or more layers (lamina). Each layer can represent a different material. FEMAP supports up to 90 layers for a laminate (180 layers are available if the laminate is symmetrical and your analysis program supports symmetrical laminates). The element shape can be Planar, three-noded triangle, four-noded quadrilateral, six-noded triangle, eight- noded quadrilateral. Some shapes are not available for all analysis programs. For each layer - Material, Orientation Angle, and Thickness. Also, Bottom Surface, Nonstructural mass/area, Bond Shear Allowable and a Failure Theory.
Connections between Aluminum profiles and composite parts are made by means of special rigid elements simulating bolted connections.

Radome is bolt joined to aircraft flange. Flange stiffness has been modeled by means of "DOF spring elements", a different stiffness value is assigned for each direction (Kx, Ky, Kz).
In order to simulate different lamination zones, the model has been divided as follows:

- Structural configuration

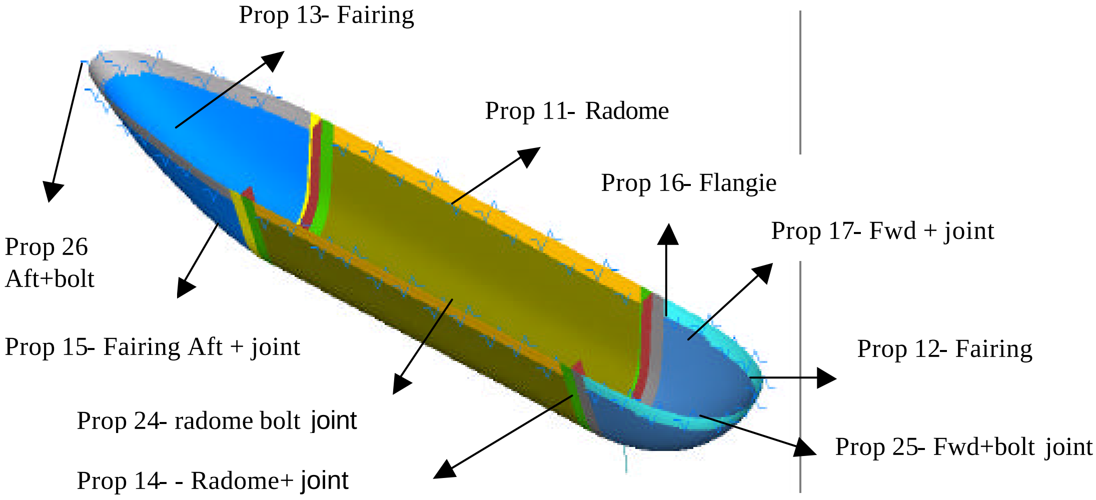

Fig.16 FEM Model

5 ANALYSIS OUTPUTS

In the following pictures the output for the worst flight condition "Load case 2" (Asymmetrical pressure distribution) can be seen. Maximum displacements and Failure index are reached on the central part (multi-layer laminate). This displacements distribution is due mainly to geometry factors, since the central wall is almost flat and consequently less stiffen than the two fairings.

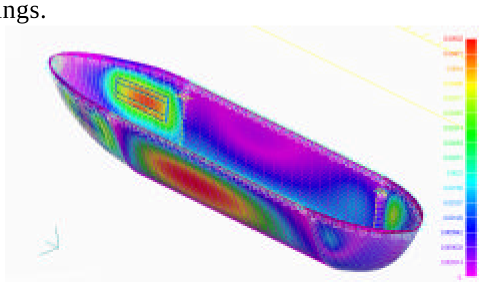

Fig.17 Displacements

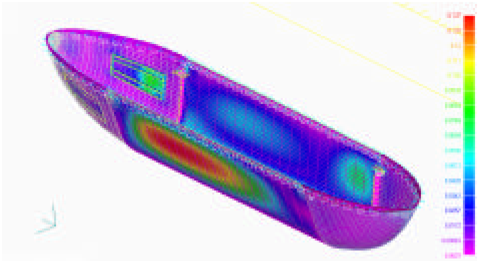

Fig.18 Failure index

6 MATERIALS MECHANICAL TESTING

Specific mechanical tests have been performed according to ASTM standard, in order to confirm the nominal mechanical values of the materials. The mechanical tests have been provided both to investigate tension properties of the skin layers sandwich materials (glass and Kevlar lay-up specimens) and for the flexural properties of the complete sandwich structures (Kevlar fiber reinforced plastic (KFRP) and honeycomb core). A METROCOM tensile machine has been used to perform both the tensile and the flexural tests.

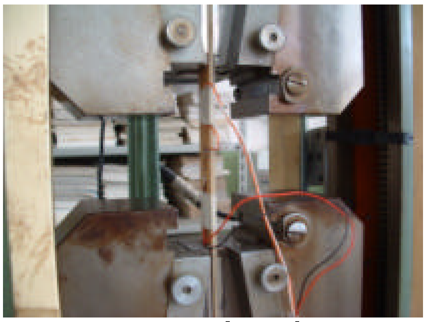
Fig.19 Tensile machine

The experimental results of the test show the complete agreement of the ultimate stress between experimental and nominal values, and they also evidence a slightly lower experimental stiffness if compared with data sheet values. These results suggest to modify the materials input data on the used numerical analysis code (FEMAP® + NASTRAN®) in order to update the structural model taking into account the real material stiffness.
Nevertheless the gap in the experimental results respect the nominal one are not as relevant as the nominal one to cause a drastic degradation of the structure mechanical behavior.[4]


Fig.20 Tensile failure

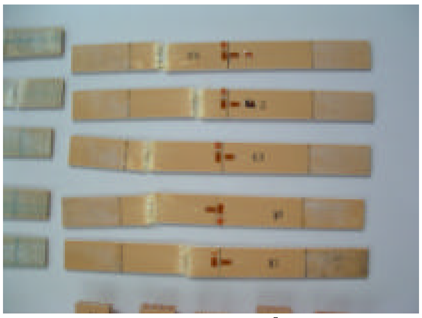
Fig.21 Samples

7 CONCLUSIONS

As a final conclusion, can be said that a complete Radome design is a multidisciplinary task involving structural and electrical studies.
Different configurations can be selected or studied depending on radar mission and radome location on aircraft.
Because of the high cost of a complete structural test verification, now a days, it is possible to qualify such kind of airborne structures by means of FEM analysis and material testing, mechanical testing on laminates can be performed in order to "certificate" and verify material characteristics. The same can be said for the bird impact where an only "numerical" verification is requested.
Laminated panel samples, with different laminate sequences, were constructed with the scope of "Electrical verification" and laboratory test were performed.

The design approach and solutions for an surveillance system underbelly radar with quite demanding electrical and mechanical features have been presented and discussed, and as a final thing, we can affirm that program success relays always on a good and well organized team work

REFERENCES

[1] Review of airborne Radomes – Dept. of electrical and computer eng. (National University of Singapore)

[2] Structural Materials Handbook – Vol2, Polymer composites (ESA PSS-03-203)

[3] Structural Materials Handbook – Vol1, Polymer composites (ESA PSS-03-203)

[4] ASTM C-393 / C-638 "Standard test method for Flexural Properties of flat sandwich constructions and tensile properties of plastics."